Shale fabric and organic nanoporosity in lower Palaeozoic shales, Bornholm, Denmark

Lucy Malou Henningsen, Christian Høimann Jensen, Niels Hemmingsen Schovsbo, Arne Thorshøj Nielsen and Gunver Krarup Pedersen

In organic-rich shales, pores form during oil and gas genesis within organic matter (OM) domains. The porosity thus differs markedly from that of conventional reservoir lithologies. Here we present the first description of shale fabric and pore types in the lower Palaeozoic shales on Bornholm, Denmark. The pores have been studied using the focused ion beam scanning electron microscope (FIB-SEM) technique, which allows for high resolution SEM images of ion polished surfaces. Shale porosity is influenced by many factors including depositional fabric, mineralogical composition, diagenesis and oil and gas generation (Schieber 2013). Here we discuss some of these factors based on a study of lower Palaeozoic shale samples from the Billegrav-2 borehole on Bornholm (Fig. 1) undertaken by Henningsen & Jensen (2017). The shales are dry gas-mature (2.3% graptolite reflectance; Petersen *et al.* 2013) and have been extensively used as analogies for the deeply buried Palaeozoic shales elsewhere in Denmark (Schovsbo *et al.* 2011; Gautier *et al.* 2014).

The Danish lower Palaeozoic shale gas play was tested by the Vendsyssel-1 well drilled in northern Jylland in 2015. Gas was discovered within a *c.* 70 m thick gas-mature, organic-rich succession (Ferrand *et al.* 2016). However, the licence was subsequently relinquished, due to a too low gas content. The present study confirms a close similarity of pore development between the shales on Bornholm and in the Vendsys-
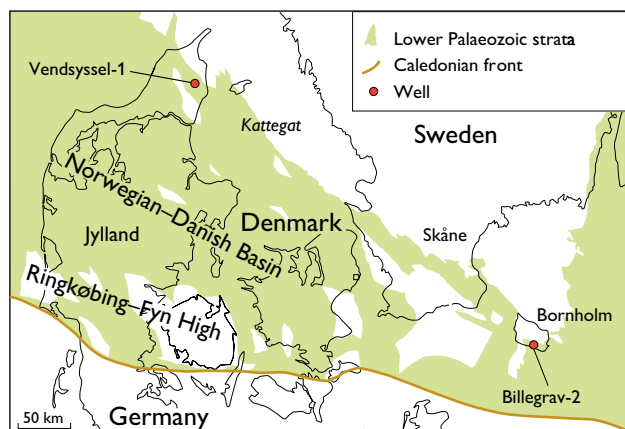
sel-1 indicating a high porosity within this stratigraphic level throughout the subsurface of Denmark. However, the rather different development of porosity in the different shale units presents a hitherto neglected aspect of the Palaeozoic gas play in Denmark.

Methods

Ten samples were selected for thin section and nanoscopic pore analyses based on a screening of 30 samples from the Billegrav-2 borehole (Fig. 2). Total organic carbon (TOC) was determined by measuring CO_2 evolved from the

Fig. 1. Distribution of lower Palaeozoic strata and wells mentioned in the text. Modified from Schovsbo *et al.* (2011).
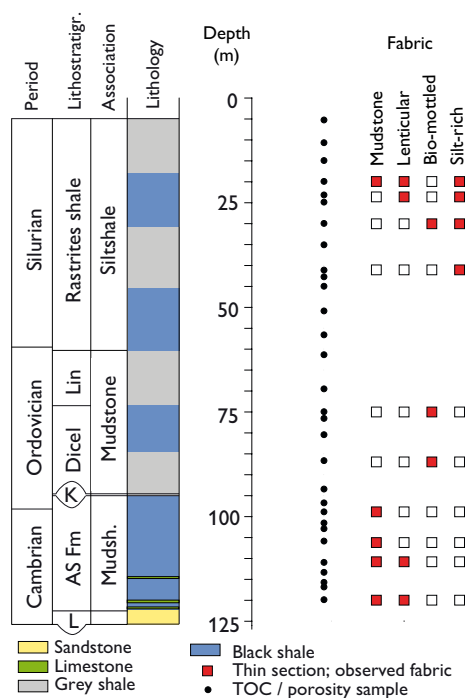

Fig. 2. Stratigraphy of the Billegrav-2 core and overview of samples and fabric types. Modified from Schovsbo *et al.* (2011). Facies associations in the interval 35–125 m are adopted from the Billegrav-1 well described by Pedersen (1989); above this level the association is based on the present text. **AS Fm**: Alum Shale Formation. **Dicel**: Dicellograptus shale. **K**: Komstad Limestone. **Lenticular**: Lenticular clast-rich mudstone. **Lin**: Lindegård Mudstone. **Lithostratigr**: Lithostratigraphy. **L**: Læså Formation. **Mudsh**: Mudshale. Fabric types: see text.
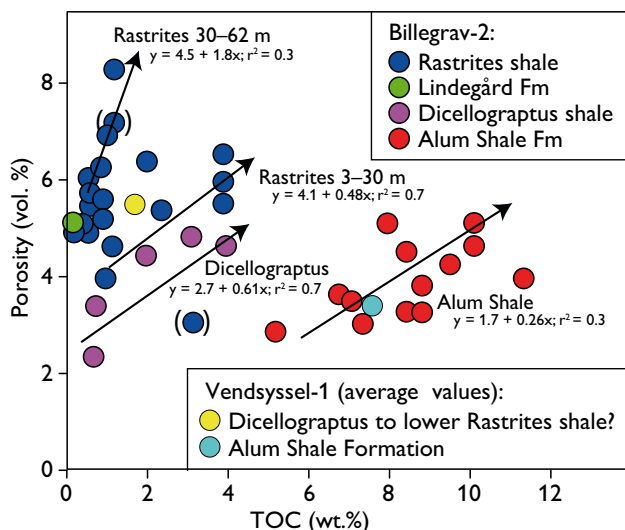
Fig. 3. Total organic carbon (TOC) content versus porosity. Arrows represent positive correlation trends (significant at a calculated probability of 0.1) within the stratigraphical units. Points in brackets represent data omitted in the correlations. Data from Vendsyssel-1 are wire-line, log-derived average values (Ferrand *et al.* 2016).

combustion of acid pre-treated samples at 1300°C. Porosity was measured in a double-chambered helium porosimeter at the Geological Survey of Denmark and Greenland. Thin sections with a thickness of about 20 μm were prepared by Pelcon Material & Testing Aps. The SEM imaging of nano- to microscale porosity was performed on cross-sections that were milled and surface polished using a focused ion beam (FIB) at the Technical University of Denmark. In order to minimise erosion of the ion-cut surface, the selected cross-section site was protected with a 3 μm thick layer of platinium. No coating of the imaged surfaces was applied.

Results

Each of the stratigraphical units shows a statistically significant correlation between TOC and porosity (Fig. 3). The Rastrites shale at 30–62 m in the borehole is the most porous shale and is characterised by the highest ratio between TOC and porosity, whereas the Alum Shale is the least porous shale, characterised by the lowest ratio between TOC and porosity (Fig. 3). The Dicellograptus shale plots between these trends together with samples from the upper 30 m of the Rastrites shale (Fig. 3).

Four shale fabrics are distinguished: (1) a dark-coloured mudstone fabric with high concentrations of OM and pyrite, (2) a lenticular clast-rich mudstone fabric, (3) a silt-rich mudstone fabric and (4) a bio-mottled mudstone fabric.

The dark-coloured mudstone fabric was observed in five samples and it is the dominant fabric in the Alum Shale. The fabric comprises a clay-dominated mudstone with variable silt-content that sometimes contains sand-sized authigenic barite (Fig. 4A). The dark colour is due to high contents of dispersed OM and pyrite. This fabric is attributed to a generally slow settling of particles in a low-energy depositional environment.

The lenticular, clast-rich mudstone fabric is seen in four samples from the Alum and Rastrites shales (Fig. 2). The content of OM and pyrite is highest in the dark grey samples and lowest in the pale grey samples (Fig. 4A). The typical lenticular clasts range in size from 500 μm to more than 2 mm and are composed of clay and silt-sized material. On a macroscopic scale, the lenticular clasts create a laminated appearance to the shale. The clasts are interpreted as deposited during episodic increases in energy in an otherwise low-energy environment.

The silt-rich mudstone fabric (Fig. 4B) shows varying concentrations of disseminated silt grains and is observed in four samples from the Rastrites shale (Fig. 2). More dense accumulations of silt grains in laminae and streaks are typically carbonate cemented. The fabric is assumed to be connected to episodic higher-energy currents in the otherwise low-energy depositional environment.

The bio-mottled mudstone fabric (Fig. 4C) occurs in three samples from the Dicellograptus and Rastrites shales. The fabric contains low amounts of OM that also tends to be irregularly distributed, both across and along the bedding planes. The distribution reflects the activities of deposit-feeding organisms. The fabric is interpreted as deposited in a more oxic marine environment characterised by low OM levels and presence of infaunal organisms.

Pores related to the OM vary from simple isolated pores to large pore populations with internally complex structures. Isolated pores are usually discrete and equant in shape and can occur both widely disseminated and in more dense populations (Figs 4D, E). They also occur in OM occupying the space between individual pyrite crystals in framboids (Figs 4F, G). The pore-size is usually <100 nm. More dense populations of <50 nm-sized, foam-like pores are also observed. This pore type seems to populate entire OM domains, but may also be surrounded by non-porous zones in presumably coherent OM domains. A third pore type consists of highly irregular pores with complex internal sub-parts (Fig. 4H). This type has a stalactite-like texture with irregular and serrated internal pore surfaces and may have internal fibrous textures resembling wood wool.

Pores related to the inorganic particles are mainly associated with irregularly shaped grains of quartz and pyrite (Fig. 4I). These pores usually appear as discontinuous slits along parts of the grain surface or as curved embayments into the

Fig. 4. Micrographs of different mudstone fabrics and pores recognised in the Palaeozoic shales. **A**: Dark coloured mudstone fabric intercalated with laminae of lenticular clast-rich mudstone fabric, 119.78–119.80 m (Alum Shale Formation). **B**: Silt-rich mudstone fabric with normal grading, 41.15–41.17 m (Rastrites shale). **C**: Biomottled mudstone fabric, presumably *Chondrites,* 86.68–86.70 m (Dicellograptus shale). Organic pores: **D**: Rounded pores, 74.77–75.01 m (Dicellograptus shale). **E**: Sub-rounded pores, 24.78–24.80 m (Rastrites shale). **F**: Subrounded to rounded pores in pyrite, 115.63–115.65 m (Alum Shale Formation). **G**: Subrounded to rounded pores in pyrite, 115.63–115.65 m (Alum Shale Formation). **H**: Irregularly shaped and complex pores, 24.78–24.80 m (Rastrites shale). Inorganic pores. **I**: Irregularly shaped pores surrounding silt- to clay-sized grains, 115.63–115.65 m (Alum Shale Formation).
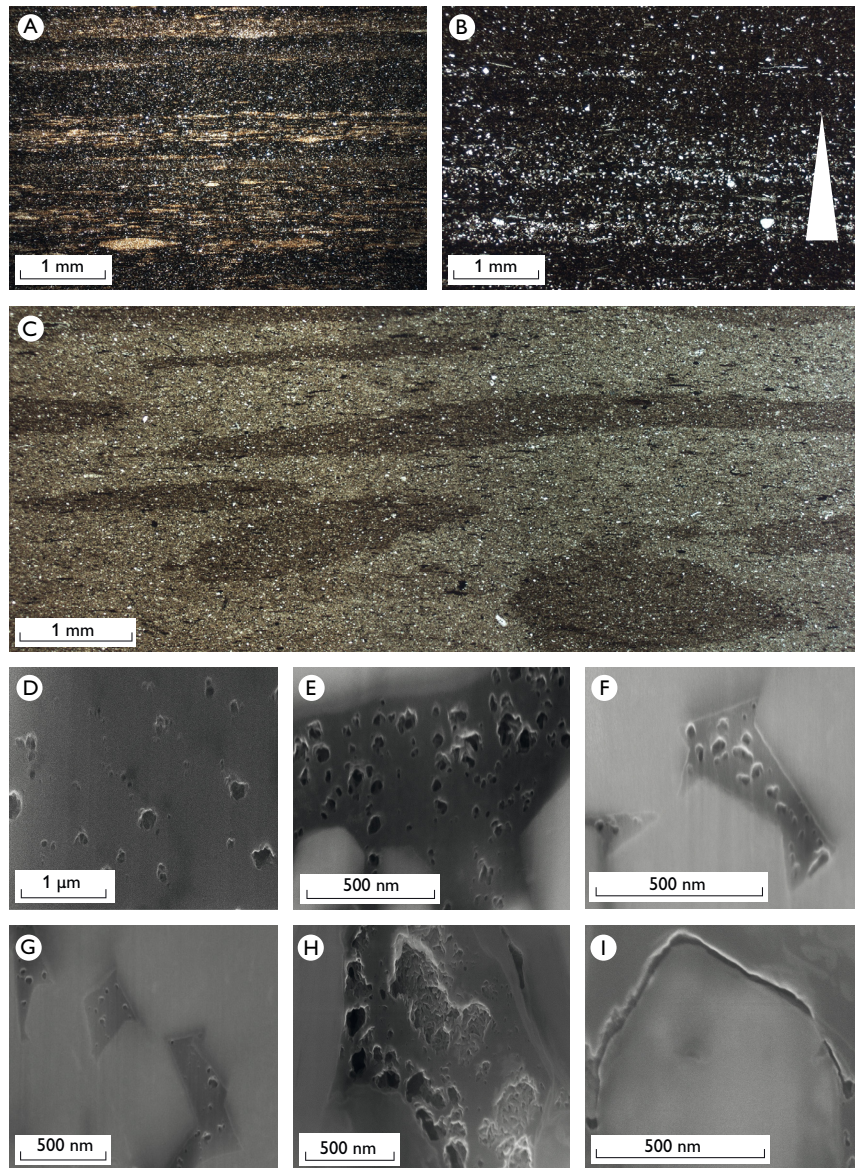
grain, and they are up to several 100 nm long. Other pore types primarily related to inorganic particles are dissolution pores that occur where matrix minerals have become partly dissolved (Fig. 4I). This pore type occurs only along the edges of carbonate minerals, and the pores tend to be elongated and irregularly shaped.

Discussion

The variable correlation between the TOC content and porosity for the Alum, Dicellograptus and Rastrites shales indicates that pores in both organic and inorganic matter contribute to the total porosity. Within each shale unit the TOC content correlates with porosity suggesting that pores hosted in organic matter are dominant in all units but with additional contributions from inorganic porosity. A higher contribution of inorganic interparticle pores is seen in the Dicellograptus and Rastrites shales that add to the overall more porous nature of these shales (Fig. 3). The Dicellograptus and Rastrites shales belong to the mudstone and siltstone associations of Pedersen (1989) whereas the Alum Shale belongs to the mud-shale association (Fig. 2) and apparently the lithofacies was the main controlling factor of the porosity development.

SEM images show that the porosity predominantly occurs within amorphous OM domains intermingled with the inorganic matrix minerals, rather than as inter-particle pores between the matrix minerals. However, not all OM domains contain pores and those that do exhibit considerable variation in quantity, distribution and size of pores.

The presence of OM in the interparticle spaces cannot be explained entirely by the processes of admixing and subsequent compactional deformation of organic and inorganic

particles (cf. Kennedy *et al.* 2002). Instead, it appears that secondary OM migrated into interparticle spaces during maturation. This interpretation is supported by observations of well-connected viscous-like OM domains, which fill the spaces between matrix minerals. The dominant clay mineral in all the samples is illite (cf. Pedersen 1989), which was either a detrital mineral or formed after diagenetic transformation of smectite during burial maturation. It may be assumed that an early migration of secondary OM occurred during the temperature interval, which matches the diagenetic transformation of the clay minerals. This relationship between secondary OM and diagenetically formed illite was also observed by Schieber (2013) in gas-mature samples from the Devonian Marcellus Shale in North America. Loucks *et al.* (2012) suggested that most smectite is transformed to illite during early catagenesis, which supports the observation of presumed migrated OM as interparticle fill.

Comparison with Vendsyssel-1

One of the discouraging results of the Vendsyssel-1 well was the low porosity and the unfavourable pore distribution in the shales (Ferrand *et al.* 2016). The average TOC content and porosity in the Vendsyssel-1 well are within the same range as those measured in the Billegrav-2 core (Fig. 3). SEM images of the Alum Shale from the Vendsyssel-1 well show both non-porous OM in the mudstone fabric and porous OM of presumed secondary origin intermingled with clay minerals (Ferrand *et al.* 2016) similar to the observations from the Billegrav-2 core.

The similarity suggests that the lower Palaeozoic shales known from Bornholm are valid analogues for the deeply buried Palaeozoic shales in Denmark. However, the rather different porosity development in the individual shale units presents a hitherto neglected aspect of the Palaeozoic gas play in Denmark.

Conclusions

The study shows that the porosities of the lower Palaeozoic shales are related to both organic and inorganic matter. The dominating porosity types in all stratigraphical units are those observed within organic matter. A clear relationship between shale fabric and organic nanoporosity has been ob-
served in the lower Palaeozoic shales and this indicates that shale composition, depositional environment, and diagenesis have all influenced the porosity development. The TOC : porosity relationships in the Vendsyssel-1 well are nearly identical to those observed in shales from Bornholm indicating a high porosity. The Alum Shale is a low porous but TOC-rich shale whereas the two other shale units studied are low in TOC but relatively porous. This observation adds another variable factor to the Danish shale gas play (cf. Gautier *et al.* 2014).

References

Ferrand, J., Demars, C. & Allache, F. 2016: Denmark – L1/10 Licence relinquishment recommendations report. Total E&P, Memo 1–9 Available from: *http://www.ft.dk/samling/20151/almdel/efk/bilag/353/1651289.pdf.* Verified 17.01.2018.

Gautier, D.L., Schovsbo, N.H. & Nielsen, A.T. 2014: Resource potential of the Alum Shale in Denmark. Unconventional Resources Technology Conference (URTeC), 25–27 August 2014, Denver Colorado. SPE-2014-1931754-MS. 10 pp.

Henningsen, L.M. & Jensen, C.H. 2017: A petrographic analysis of pores and their distribution in Palaeozoic organic-rich shale (the Alum Shale Formation, the Dicellograptus shale, and the Rastrites shale) from the Billegrav-2 core, Bornholm, Denmark, 110 pp. Unpublished Master thesis, University of Copenhagen. GEUS Report Files **34178** and **34179**).

Kennedy, M.J., Pevear, D.R. & Hill, R.J. 2002: Mineral surface control of organic carbon in black shale. Science **295**, 657–660.

Loucks, R.G., Reed, R.M., Ruppel, S.C. & Hammes, U. 2012: Spectrum of pore types and networks in mudrocks and a descriptive classification for matrix-related mudrock pores. AAPG Bulletin **96**, 1071–1098.

Pedersen, G.K. 1989: The sedimentology of Lower Palaeozoic black shales from the shallow wells Skelbro-1 and Billegrav-1, Bornholm, Denmark. Bulletin of the Geological Society of Denmark **37**, 151–173.

Petersen, H.I., Schovsbo, N.H. & Nielsen, A.T. 2013: Reflectance measurements of zooclasts and solid bitumen in Lower Palaeozoic shales, southern Scandinavia: correlation to vitrinite reflectance. International Journal of Coal Petrology **114**, 1–18.

Schieber, J. 2013: SEM observations on ion-milled samples of Devonian black shales from Indiana and New York: the petrographic context of multiple pore types. AAPG Memoir **102**, 153–171.

Schovsbo, N.H., Nielsen, A.T., Klitten, K., Mathiesen, A. & Rasmussen, P. 2011: Shale gas investigations in Denmark: Lower Palaeozoic shales on Bornholm. Geological Survey of Denmark and Greenland Bulletin **23**, 9–12.

Authors' addresses

L.M.H., *Energinet, Tonne Kjærsvej 65, DK-7000 Fredericia, Denmark;* Email: *lucymalou@gmail.com.*

C.H.J., *Region Sjælland, Alleen 15, DK-4180 Sorø, Denmark.*

N.H.S. & G.K.P., *Geological Survey of Denmark and Greenland, Øster Voldgade 10, DK-1350 Copenhagen K, Denma*rk.

A.T.N., *Department of Geosciences and Natural Resource Management, University of Copenhagen. Øster Voldgade 10, DK-1350 Copenhagen K, Denmark.*